

8 Appendix

8.1 Labelled data content

{

"content": "\nMicroporous and Mesoporous Materials 78 (2005) 181-188\nwww.el
sevier.com/locate/micromeso\nMeso/macroporous AlPO-5 spherical macrostructures tailored by resin templating Valeri Naydenov a,*
Lubomira Tosheva a,1, Oleg N.
Antzutkin b,*
Division of Chemical Technology,
Lulea University of Technology,
S-971 87 Lulea , Sweden
Received 22 June 2004;
received in revised form 4 October
2004; accepted 5 October
2004 Available online 30 November
2004\nAbstract\nA multi-step procedure for the preparation of meso/macroporous AlPO-5 spherical macrostructures using cation exchange resin beads as macrotemplates is presented. Firstly, aluminum species were introduced into the resin beads by ion exchange resulting in a resin-aluminum composite. Thereafter, the resin-aluminum composite was mixed with TEAOH, H3PO4 and distilled water and hydrothermally treated at 150 °C to yield resin-AlPO-5 composite. Finally, the resin was removed by calcination leaving behind self-bonded AlPO-5 spheres. The product AlPO-5 macrostructures were thoroughly characterized by SEM, XRD, nitrogen adsorption measurements, 31P and 27Al solid state NMR spectroscopy. The influence of various components of the synthesis mixture on the crystallinity, phase purity and stability of the AlPO-5 spheres was systematically studied. Samples prepared for different treatment times using the initial synthesis composition that gives spheres of the highest quality were used to study the crystallization process within the resin.\nElsevier Inc. All rights reserved.\nKeywords: AlPO-5; Hierarchical porosity; Spheres; Macrotemplate; Ion-exchange resin\nIntroduction\nMolecular sieve materials have found wide use in a large number of industrially important areas such as chemical separation, adsorption and heterogeneous catalysis. For certain applications however, the small pore size of zeolites (micropores) may cause diffusion limitations. Also, zeolites are usually synthesized as powders, which are difficult to handle and post-synthetic\n*

Corresponding authors. Tel.: +46 920491199. E-mail address: oleg.antzutkin@ltu.se (O.N. Antzutkin).1 Present address: LMM, UMR-7016 CNRS, ENSCMu, Université de Haute Alsace, rue Alfred Werner, F-68093 Mulhouse Cedex, France.2 Present address: Va "xjo" University, Universitetsplatsen 1, S-351 95 Va "xjo", Sweden.\n1387-1811/\$ - see front matter © 2004 Elsevier Inc. All rights reserved.doi:10.1016/j.micro
meso.2004.10.008\nmodifications to obtain the zeolites in macroscopic forms are needed. During the last years, a lot of research has been directed towards the development of synthetic procedures that tailor the pore structure and the macroscopic shape of zeolites. A number of molecular sieve bodies with hierarchical porosity providing fast transport to and from the zeolite pores as well as with macro-shapes that meet the operating conditions for a particular application have been synthesized using macrotemplates. The macrotemplate acts as a mold determining the macroscopic shape of the product material, whereas the removal of the macrotemplate after synthesis creates a secondary porosity in the meso and/or macropore range. Thus, zeolites in forms of monoliths [1-4], fibers [5], hollow capsules [6], sponge-like architectures [7] and self-standing tissues [8] have been synthesized using starch [1], latex beads [2], mesoporous silica spheres [3,6], polyurethane foams [4], bacterial\nV. Naydenov et al. / Microporous and Mesoporous Materials 78 (2005) 181-188\nthreads [5], cellulose acetate membranes [7] and woodcellular structures [8] as templates. Microporous aluminophosphate solids are another important class of molecular sieve materials that have a three-dimensional framework built up of alternating(AlO4) and (PO4) units. AlPO-5 (AFI type structure) is the most studied member of this family. The influence of synthesis composition, chemicals used and the heating procedure on the AlPO-5 crystallization have been discussed in a number of papers [9-18]. However to the best of our knowledge, the accessibility of aluminophosphate molecular sieves for preparation of self-bonded macro-shaped bodies have not yet been explored. Here, we report on a procedure for tailoring spherical meso/macroporous AlPO-5 macrostructures using cat-ion exchange resins as macrotemplates.

The procedure is a further development of the resin-templating method used for the preparation of silicalite-1 [19] and zeolite[20,21] molecular sieve macrostructures using anion exchange resins. However, this type of resin is not applicable for AlPO-5 macrostructure synthesis since positively charged aluminophosphate species are present in AlPO-5 synthesis solutions [22]. In addition, the crystal-lization mechanism of AlPO-5 within the resin was studied in detail by ³¹P and ²⁷Al solid state NMR.

Experimental section

Fig. 1 shows a schematic representation of the whole procedure used in this work for the preparation of the meso/macroporous AlPO-5 spherical macrostructures through resin templating.

2.1. Preparation of the resin-Al composites

A macroreticular Amberlite IRA-200 cation exchange resin (mesh size 16–50, Sigma) was used in all experiments. The ionic form of the resin was reversed from Na⁺ to H⁺ by passing a 10 wt.% HCl solution through an ion exchange column loaded with the resin. A large batch of resin-Al composites was prepared by mixing the resin (H⁺ form) with a 0.1 M tetraethyl-ammonium chloride hydrate (TEACl, Aldrich), dissolved in an aluminum chlorohydrate solution diluted 10 times (Locron L, 23.4 wt.% Al₂O₃, OH/Al = 2.5, Hoechst) in a weight ratio resin to solution of 1:10, followed by a treatment in an oil bath at 100 °C under reflux for 24 h. The resin-Al composite was separated after the synthesis by decanting, rinsed repeatedly with distilled water and dried at room temperature. The amount of aluminum (22.9 wt.%) exchanged into the resin (calculated as Al₂O₃) was determined gravimetrically by the weight difference between resin-Al composites dried at 105 °C and the beads calcined at 600 °C.

Preparation of AlPO-5 macrostructures

Synthesis mixtures containing ortho-phosphoric acid(85%, Merck), distilled water, tetraethylammoniumhydroxide (TEAOH, 20 or 35 wt.% aqueous solutions, Sigma) and resin-Al composites in quantities to yield molar compositions TEAOH:Al₂O₃: H₂O, where x = 1.5, y = 0.9, z = 50, were prepared. The water gained during storage or the tetra-ethylammonium ion present in the resin-Al composite from the initial treatment of the resin with alumina, were not taken into account in the calculations.

The mixtures were hydrothermally treated in autoclaves at 150 °C for treatment times between 2 and 24 h. After hydrothermal treatment, the resin-AlPO-5 composite was separated from the mother liquor by decanting, rinsed repeatedly with distilled water and dried at room temperature. The dried composite was finally calcined at 600 °C for 20 h after heating to this temperature at a rate of 1 °C min⁻¹.

Characterization

A Philips XL 30 scanning electron microscopy (SEM) was used to study the morphology of the samples. Nitro-a Micromeritics ASAP 2010 instrument at 196 °C after nitrogen adsorption/desorption isotherms were obtained with degassing the samples at 300 °C overnight prior to analysis. Specific surface area was calculated with the BET equation. Pore size distributions were determined from the desorption branch of the isotherms using the BJH method. Micropore surface areas and micropore volumes were determined by the t-plot method and total pore volumes were obtained from the volume adsorbed at a relative pressure of 0.995. Crystalline phases were identified with XRD using CuKα radiation. The pH of the mother liquors was measured with a pH meter 691 (Metrohm). Solid-state ³¹P magic-angle-spinning (MAS) NMR spectra were recorded on a Varian/Chemagnetics Infini-nity CMX-360 ($B_0 = 8.46$ T) spectrometer using the single-pulse experiment with proton decoupling. The ³¹P operating frequency was 145.73 MHz. In the single pulse experiment, the ³¹P 90° pulse duration was 5.0 ls and the nutation frequency of protons during decoupling was $\pi/2p = 100$ kHz. 16 signal transients spaced by a relaxation delay of 60 s were accumulated. Calcined powder samples (ca. 30–35 mg, additionally dried at 350 °C for 3 days in order to allow quantitative measurements of phosphorus) were packed in zirconium dioxide double bearing 4 mm rotors. All ³¹P solid state MAS NMR spectra were recorded at room temperature.

²⁷Al MAS NMR experiments were performed at room temperature on a Varian/Chemagnetics Infinity-600 (University of Warwick, UK) spectrometer at ²⁷Al carrier frequency of 156.37 MHz in 3.2 mm zirconium dioxide rotors at a spinning frequency of 18,000 ±10 Hz. The duration of the 30 -excitation pulse was 0.5 ls. 128 signal transients were accumulated with a repetition time of 1 s. Samples were externally referenced on a powder YAG sample [24], which was also used for the tuning of the magic angle.\n 3. Results and discussion\n Fig. 2 shows a SEM image of the initial resin beads used as macrotemplates (Fig. 2a) and images of the product particles (Fig. 2b-f) obtained at the different steps of the procedure depicted in Fig. 1. According to SEM, the first step of the procedure, namely the introduction of aluminum within the resin does not cause changes into e.g. the size and/or shape of macrotemplates (Fig. 2b). The resin-AlPO-5 composite particles obtained in the next step of the procedure were also similar in size and shape to the original resin beads but with somewhat rougher surfaces due to AlPO-5 agglomerates exposed on the surface (Fig. 2c). The calcined AlPO-5 spheres were similar in shape with a slightly reduced size compared to the original resin beads (Fig. 2d). Some of the particles were cracked and even broken. The sphere surfaces were rough with micrometer-sized voids and cavities (Fig. 2e). No such voids were observed in the sphere interiors. The AlPO-5 spheres were built up of fine nano-particles as shown in Fig. 2f. This observation\n is not surprising considering the fact that AlPO-5 crystallizes within the resin pores, which have an average size of ca. 100 nm [25]. This may explain the absence of micrometer-sized crystals with well defined AlPO-5 hexagonal morphology. The described procedure for the preparation of AlPO-5 spherical macrostructures differs significantly from the conventional AlPO-5 syntheses [9] reported in literature, as well as from the procedures used for the synthesis of silicalite-1 [19] or zeolite [20,21] macro-structures by resin templating. The experiments to prepare AlPO-5 macrostructures by direct treatment of cation exchange resins with AlPO-5 synthesis solutions did not give satisfactory results.

Particles of limited crystallinity often accompanied by a loss of macroshape were obtained. The problem of disintegration of the macroshape was solved by insertion of aluminum pre-cursor within the resin prior to AlPO-5 synthesis. This preliminary step ensures that the AlPO-5 crystallization is realized only within the resin pore structure and therefore an easy recovery of the product spheres due to the absence of bulk crystallization. Further, the presence of TEA⁺ in the solution used for Al ion exchange was essential for the AlPO-5 synthesis. The exact role of the TEA⁺ is not clear at this point of the study. However, when a resin-Al composite was prepared in the absence of TEACl and used for AlPO-5 synthesis the products obtained upon calcinations were powders rather than beads. This indicates that the TEA⁺ might “fix” the aluminum species within the resin to ensure homogeneous AlPO-5 crystallization within the macrotemplate.\n Further, structural and macroscopic characteristics of the product samples prepared with different initial compositions were studied and results are given in Table 1. The duration of the hydrothermal treatment for all samples was 10 h at 150 °C. The objective of the present work was to synthesize stable AlPO-5 spheres of high crystallinity. Therefore, the quality of the samples was evaluated by the degree of crystallinity, purity of AlPO-5 and by the mechanical stability of the product AlPO-5 spheres. Although the mechanical stability of the macrostructures was not tested, obtained particles were stable and could withstand various laboratory manipulations. However it should be mentioned, that AlPO-5 spheres were easier to grind (e.g. prior XRD or NMR studies) compared to Silicalite-1 and zeolite Beta macrostructures prepared by resin templating[19,20]. A possible explanation might be the difference in the amount of solid material within resin-molecular sieve composites obtained after synthesis, which decreases from zeolite Beta (56 wt.%) through Silicalite-1 (44 wt.%) to AlPO-5 (26 wt.%). As evident from the data presented (Table 1) the best results in terms of crystallinity, purity and mechanical stability were obtained for sample 4 and this synthesis mixture was used to prepare\n 184 V. Naydenov et al. / Microporous and Mesoporous Materials 78 (2005) 181–188\n

Fig. 2. SEM images of the cation exchange resin beads (a) and the product particles (b-f) synthesized from system with molar composition 2TEAOH : Al2O3:1.2P2O5:100H2O after hydrothermal treatment at 150 °C for 10 h. Table 1 Synthesis of AlPO-5 macrostructures from different system compositions
 Sample Molar composition TEAOH Al2O3 P2O5 H2O
 12345678910f11121314
 2.02.02.02.01.52.53.03.52.02.02.
 02.02.01.001.001.001.001.001.
 001.001.001.001.001.001.001.001.001.
 01.001.101.201.301.201.201.201.201.
 201.201.201.201.201.201.201.201.201.
 10010010010050150200300500
 According to XRD; Am-amorphous; T-tridymite; Im-impurities.b Visually.c Yellowish.d Slightly gray.e Deteriorated.f Sample prepared with 35 wt.% TEAOH.
 Product characteristics
 AmAmAm + AlPO-5AlPO-5TIm + AmAm + traces of AlPO-5AmAmAlPO-5 + TAlPO-5 + ImAlPO-5 + ImAlPO-5 + Im + AmIm + AmMacro-shapeb
 SpherescSpherescSpherescSpheresSphe
 resSpherescSpherescSpheresSphe
 spherescsPowder + spherescsPowder + spheresSpheresSpheresSpheresSpheres
 nsamples for different treatment times to study the AlPO-5 crystallization mechanism within the resin.
 Fig. 3 shows XRD patterns of series of calcined samples synthesized using the same synthesis mixture as
 V. Naydenov et al. / Microporous and Mesoporous Materials 78 (2005) 181–188
 Fig. 3. XRD patterns of the calcined samples obtained from the system with molar composition 2TEAOH:Al2O3:1.2P2O5:100H2O at 150 °C for various treatment times.
 sample 4 (Table 1) and prepared with duration of the hydrothermal treatment between 2 and 24 h. The initial resin-Al composite beads used in these experiments were from the same batch. The sample prepared using 2 h of treatment was completely amorphous. AlPO-5 peaks of very low intensity were detected in the sample obtained after 4 h of treatment. The intensity of the AlPO-5 peaks further increased with an increase in the time of hydrothermal treatment and the sample prepared for 10 h was highly crystalline pure AlPO-5. In addition to the AlPO-5 phase, impurities of another unidentified crystalline phase

(designated with arrows on the Figure) were also present in the samples treated for 5, 6 and 8 h. Surprisingly, prolonging the hydrothermal treatment to 12 and 24 h lead to AlPO-5 spheres containing impurities of crystalline phases most likely the same as detected for shorter treatment times. Since the trend shown in Fig. 3 is rather unexpected the reproducibility of the results was confirmed by the repetition of the synthesis. The changes in the pore structure of product macro-structures with the time of treatment were studied by nitrogen adsorption, BET surface areas, micropore surface areas and volumes and total pore volumes are listed in Table 2. The values for the calcined initial resin-alu-mina composites are also included in the Table for a comparison. The size of those spheres was substantially reduced upon calcination and this might explain the lower total pore volume of this sample. Though the values vary, the general trend is an increase in the BET surface area and porosity of the calcined samples synthesized from system with molar composition 2TEAOH:Al2O3:1.2 P2O5:100H2O at 150 °C altering the duration of the hydrothermal treatment.
 Sample
 BET surface area, SBET(μm²)(m² g⁻¹)
 Micropore surface area, (μm²)S1 (m² g⁻¹)
 Micropore volume, (μm³)V1 (cm³ g⁻¹)
 Al spheres2 h4 h5 h6 h8 h10 h12 h24 h
 5711085102304172289296265
 881028183
 n98214227184
 0.0030.0020.0040.0130.0870.0460.102
 0.1080.087 nTotal
 pore volume, Vp(μm³)(cm³ g⁻¹)
 0.2380.8160.8010.8640.4370.6970.426
 0.4010.409 n face area, micropore surface area and volume and a decrease in the total pore volume with increased time of treatment. The samples prepared using 6 and 8 h of treatment show values that do not fit into this trend. The reason might be that according to XRD, AlPO-5 becomes the predominant phase in the 6 h sample and thus the changes in the structure of the inorganic material within the resin are most intense at this time interval of treatment (6–8 h). Different complex species containing Al or binuclear Al centers with H3PO4 or H2PO4 and H2O molecules as ligands showing P chemical shifts in this range have been reported in literature [27–29]. However, the specification of the short range solid structure judging only from the 31P solid state NMR would be highly speculative. After 5 h of hydrothermal treatment a new peak (with a linewidth of ~18.6 ppm) at ca. ~29 to ~30 ppm appeared on the top of the broad peak (at ~27 ppm).

This indicates that a new material with more ordered structure (P sites with more uniform local chemical environment) is forming in this sample. Chemical shift δ to ~ 30 ppm is in the range characteristic for tetrahedral P sites in the framework of microporous materials [30,31]. In support to this, AlPO-5 peaks were also observed in the XRD pattern of sample 5 h (Fig. 3(5 h)). In the spectra of the samples treated for 6 (not shown) and 8 h the peak at $\delta = 29$ to ~ 30 ppm dominates over the broad component that corresponds to the initial amorphous solid. According to the ^{31}P NMR, after 10 h of hydrothermal treatment, the conversion from amorphous to a poly-crystalline material is completed. Only slight changes in the line shapes can be noticed in the spectra of the samples prepared for 12 and 24 h (not shown) of hydrothermal treatment. The spectra of samples (10 h), (12 h) and (24 h) are characterized by a resonance line, which might actually be composed of two overlapping peaks, ca. $\delta = 30$ and ~ 31 ppm with total line-width of ca. $\Delta\delta = 18.5$ ppm. This resonance line width is somewhat broader than what is usually observed for highly polycrystalline phosphorus-containing materials. A large part of the line broadening is probably due to interaction of P-spins with ^{27}Al nuclei (spin $5/2$, 100% natural abundance). However, the assignment of the ^{31}P peak(s) at $\delta = 30/\sim 31$ ppm (together with the line-widths) to microporous AlPO-5 is in agreement with the results previously reported in the literature for the dehydrated AlPO-5 phase [30–32]. Integral intensities of the ^{31}P resonance lines in Fig. 5 can be used for quantitative estimation of the phosphorus content (in wt %) for these samples. In the calculations, all ^{31}P integral peak areas (centre band waist between 20 and ~ 70 ppm, see Fig. 5) were normalized to integrated together with its spinning side bands, i.e. being the area of the peak of commercial AlPO4 (Fig. 5 bottom) with known phosphorus content (25.4 wt%). The total amount of P introduced as H_3PO_4 in the system during the sample preparation was 26.9 wt%. The P content as well as the pH of the mother liquor as a function of the duration of hydrothermal treatment are plotted in Fig. 6.

From the Figure it is seen that most of the phosphorus (ca. 25.0 wt.%) is present within the resin after the first 2 h of treatment. With an increase in the duration of the hydrothermal treatment, the P content in the spheres slowly increases and reaches a plateau at ca. 29.1 wt.% after the tenth hour of treatment. The results for P content are slightly higher than the calculated value on H₃PO₄ basis but nevertheless give values of satisfactory accuracy. These errors in P content measurements might be caused by variation of the sample weight due to water adsorbed from air by the samples during the rotor packing. It is known that anhydrous AlPO₄, which was used as a reference sample in the calculations, is a highly hydroscopic material. The pH is an important parameter in aluminophosphate syntheses, which may alter crystal size and product [11]. V. Naydenov et al. / Microporous and Mesoporous Materials 78 (2005) 181–188 [12] 1098765432 nr i ou nq n i nl r e nh t n o nm e nh t n n ni H p P content pH 048121620 n24 Duration of hydrothermal treatment/h 40 n 35 n 30 n 25 n 20 n 15 n 10 n % t n w / nt ne t n noc P Fig. 6. P content in the product spheres (estimated from ³¹P MAS NMR) and pH of the mother liquors collected after synthesis of samples obtained from system with molar composition 2TEAOH:Al2O3:1.2P2O5:10H₂O at 150 °C as a function of the duration of the hydrothermal treatment. n yield [10, 13, 16–18]. In this study, the pH values plotted in Fig. 6 are values measured outside the resin in the mother liquor, therefore they should be used with some precaution since the pH of the mother liquor might significantly differ compared to that within resin interior, where AlPO₄ actually crystallizes. The pH monitoring might give information about the transportation of e.g. P and TEA⁺ in the resin. The initial pH of the H₃PO₄, TEAOH and distilled water mixture was 3.1. During the first 2 h of treatment, the pH of the mother liquor sharply increased to 5.4, slightly decreased after 5 h of treatment and reached ca. 4.5 upon further prolongation of the treatment. It should be emphasized that although this is the pH of the mother liquor, the pH remains acidic during the whole time interval explored, whereas for conventional syntheses the final pH is about neutral [10].

In the literature the initial increase in the pH during the syn-thesis is considered as an indication that the amount of the free phosphoric acid is decreasing [13,16]. This is most likely the case in our approach as well, since the ini-tial increase of the pH (2 h of treatment) correlates wellwith the large amount of P for this sample measuredby quantitative 31P NMR. In addition, the fact that the pH remains in the acidic range, suggests that the TEA⁺is also transported into the resin already at the beginningof the synthesis.Fig. 7 shows single-pulse 27Al MAS NMR spectra of the calcined resin-Al composites (denoted as Alspheres), commercial AlPO₄ and selected spectra fromseries of samples obtained varying the duration ofhydrothermal treatment discussed in Fig. 5 and Fig. 6.These spectra were recorded for as received samplesi.e. without additional drying prior to measurements to remove adsorbed water. Aluminum sites in the cal-cined resin-Al composite have three predominant typesof chemical environment, characterized by broad peaksat ca. 60, 40 ppm (tetrahedral coordination) and ca.\n (24 h)\n (10 h)\n (6 h)\n(2 h)\ncommercial AlPO₄\n Al spheres\n100\n75\n 50\n25\n 0\n-25\n-50\n Chemical shift / ppm\n Fig. 7. Single pulse 27Al MAS NMR spectra of the samples obtainedfrom thesystem with molar composition2TEAOH:Al2O3:1\n .2P2O5:100H2O at 150 C for various treatment times.\n 5 ppm (octahedral coordination) (Al spheres). All thesepeaks completely disappeared after 2 h of hydrothermal(Al (V)) and about \u000013 ppm (Al (VI)) (Fig. 7(2 h)) ap-treatment, and new peaks at 45 ppm (Al (IV)), 10 ppmpeared. These new peaks are almost identical to thosein the spectrum of commercial AlPO₄ (Fig. 7). The weakbut discernible signal at about 10 ppm can be assigned to the five-coordinated aluminum according to previous re-ports [33]. With an increase in the duration of the hydro-thermal treatment all three resonance peaks becomenarrower with the peaks being sharpest for the samplesobtained after 10 h and 24 h of treatment. Also, a consi-derable shift of the 27Al-resonance peak at 45 ppm to atabout 37 ppm is noticed for the tetrahedral aluminumsites in the sample (Fig. 7(10 h)),

which was previouslyassigned to the AlPO-5 based on XRD (Fig. 4 (10 h))and 31P (Fig. 5(10 h)) results. The small fraction of octa-hedral aluminum sites in AlPO-5 (at ca. \u000012 ppm) canalso be observed, since a certain amount of water is ad-sorbed by the sample. In previous reports it has beenshown by a number of 2D 27Al-31P NMR correlationexperiments performed on water-AlPO-5 system thatthese Al (VI)-sites, which additionally coordinate twowater molecules can be correlated with 31P-signals forthe latter system, i.e. these Al (VI) sites are actually inthe AlPO-5 framework positions [34]. Therefore, both31P and 27Al NMR as well as XRD studies prove thatthe sample prepared for 10 h of hydrothermal treatmentcontains a high quality AlPO-5 phase.\n 4. Conclusions\n Highly crystalline and mechanically stable AlPO-5spheres were prepared using a cation exchange resin as\n V. Naydenov et al. /\n Microporous and Mesoporous Materials 78 (2005) 181-188\n a macrotemplate. The AlPO-5 phase crystallized in the pore structure of a cation exchange resin loaded withAl precursor species under a hydrothermal treatmentwith a mixture of H3PO4, TEAOH and distilled water.The overall molar composition of the synthesis mixtureinfluences both phase purity and sphere appearance.Best results, highly crystalline AlPO-5 spheres, were obtained using the mixture with the molar composition2TEAOH:Al2O3:1.2P2\n 05:100H2O and 10 h of hydro-thermal treatment at 150 C. The spheres synthesizedfor treatment times other than 10 h were contaminatedwith amorphous and/or other crystalline phases.The pore structure of the AlPO-5 spheres preparedfor 10 h of treatment was complex containing micro-meso- and macropores. The micropores are due to thepresence of AlPO-5, whereas the meso and macroporesemanate from the resin removal.The crystallization mechanism of AlPO-5 within theresin was extensively studied by solid state NMR.The quantitative determination of the P content withinthe solid spheres by 31P NMR indicated that P is takenup by the resin from the external solution at the begin-ning of the hydrothermal treatment (2 h). Further pro-longation ofthetreatmentleadsto structuralrearrangements of the system resulting in the crystalliza-tion of AlPO-5.

The quality of the AlPO-5 phase was evaluated by XRD, nitrogen adsorption, ³¹P, and ²⁷Al MAS NMR measurements. The procedure presented contributes to the current trends directed towards the preparation of self-bonded materials with hierarchical pore structures. The macroscopic spherical shape and the complex pore structure of the AlPO-5 spheres prepared makes them interesting for direct applications in e.g. fixed bed reactors.

Acknowledgment

We thank Prof. R. Dupree and Dr. Rusanova-Naydenova for both instrument time and assistance in operating with Varian/CMX-600 NMR instrument (Warwick University, UK). O.N.A. acknowledges Swedish Concil for planning and coordination of research (FRN) for a grant for the Varian/CMX-360 spectrometer and Foundation to the memory of J.C. and Seth M. Kempe for a grant for the TR-4 mm-MAS probe and other equipment. The partial financial support from the Swedish Research Council for Engineering Sciences (VR) is gratefully acknowledged.

References

- [1] B. Zhang, S.A. Davis, S. Mann, Chem. Mater. 14 (2002) 1369.
- [2] K.H. Rhodes, S.A. Davis, F. Caruso, B. Zhang, S. Mann, Chem. Mater. 12 (2000) 2832.
- [3] A. Dong, Y. Wang, Y. Tang, Y. Zhang, N. Ren, Y. Yue, Z. Gao, Adv. Mater. 14 (2002) 1506.
- [4] Y.-J. Lee, J.S. Lee, Y.S. Park, K.B. Yoon, Adv. Mater. 13 (2001) 1259.
- [5] B. Zhang, S.A. Davis, N.H. Mendelson, S. Mann, Chem. Commun. (2000) 781.
- [6] A. Dong, Y. Wang, Y. Tang, N. Ren, Y. Zhang, Z. Gao, Chem. Mater. 14 (2002) 3217.
- [7] Y. Wang, Y. Tang, A. Dong, X. Wang, N. Ren, W. Shan, Z. Gao, Adv. Mater. 14 (2002) 994.
- [8] A. Dong, Y. Wang, Y. Tang, N. Ren, Y. Zhang, Y. Yue, Z. Gao, Adv. Mater. 14 (2002) 926.
- [9] S.T. Wilson, B.M. Lok, C.A. Messina, T.R. Cannan, E.M. Flanigen, J. Am. Chem. Soc. 104 (1982) 1146.
- [10] B.L. Newalkar, B.V. Kamath, R.V. Jasra, S.G.T. Bhat, Zeolites 18 (1997) 286.
- [11] M.Z. Yates, K.C. Ott, E.R. Birnbaum, T.M. McCleskey, Angew. Chem. Int. Ed. 41 (2002) 476.
- [12] G. Finger, J. Richter-Mendau, M. Bülow, J. Kornatowski, Zeolites 11 (1991) 443.
- [13] X. Ren, S. Komarneni, D.M. Roy, Zeolites 11 (1991) 142.
- [14] O. Weiβ, G. Ihlein, F. Schuth, Micropor. Mesopor. Mater. 35-36 (2000) 617.
- [15] S. Mintova, S. Mo, T. Bein, Chem. Mater. 10 (1998) 4030.
- [16] T. Kodaira, K. Miyazawa, T. Ikeda, Y. Kiyozumi, Micropor. Mesopor. Mater. 29 (1999) 329.
- [17] I. Girnus, K. Jancke, R. Vetter, J. Richter-Mendau, J. Caro, Zeolites 15 (1995) 33.
- [18] H. Du, M. Fang, W. Xu, X. Meng, W. Pang, J. Mater. Chem. 7 (1997) 551.
- [19] L. Tosheva, V. Valtchev, J. Sterte, Micropor. Mesopor. Mater. 35-36 (2000) 621.
- [20] L. Tosheva, B. Mihailova, V. Valtchev, J. Sterte, Micropor. Mesopor. Mater. 48 (2001) 31.
- [21] L. Tosheva, J. Sterte, R. Fiello, G. Giordano, F. Testa (Eds.), in: Impact of zeolites and other Porous Materials on the new Technologies at the Beginning of the new Millennium, Elsevier, Amsterdam. Stud. Surf. Sci. Catal. 142A (2002) 183.
- [22] S. Prasad, S.-B. Liu, Micropor. Mater. 4 (1995) 391.
- [23] K. Karaghiosoff, Encyclopedia of Nuclear Magnetic Resonance, Wiley, New York, 6 (1996) 3612.
- [24] D. Massiot, C. Bessada, J.P. Coutures, F. Taulelle, J. Magn. Reson. 90 (2) (1990) 231.
- [25] C.E. Harland, Ion Exchange: Theory and Practice, The Royal Society of Chemistry, Cambridge, 1994, p. 28.
- [26] B.B. Johnson, A.V. Ivanov, O.N. Antzutkin, W. Forsling, Langmuir 18 (2002) 1104.
- [27] J.W. Akitt, N.N. Greenwood, G.D. Lester, J. Chem. Soc. (A) (1971) 2450.
- [28] R.F. Mortlock, A.T. Bell, C.J. Radke, J. Phys. Chem. 97 (1993) 767.
- [29] R.F. Mortlock, A.T. Bell, C.J. Radke, J. Phys. Chem. 97 (1993) 775.
- [30] D. Müller, E. Jahn, G. Ladwig, U. Haubenreisser, Chem. Phys. Lett. 109 (1984) 332.
- [31] D. Müller, E. Jahn, B. Fahlke, G. Ladwig, U. Haubenreisser, Zeolites 5 (1985) 53.
- [32] R.H. Meinhold, N.J. Tapp, J. Chem. Soc. Chem. Commun. (1990) 219.
- [33] G. Kunath-Fandrei, T.J. Bastow, J.S. Hall, C. Jaeger, M.E. Smith, J. Phys. Chem. 99 (1995) 15138.
- [34] C.A. Fyfe, K.C. Wong-Moon, Y. Huang, Zeolites 16 (1996) 50.

"connections": [

```
{
    "toId": 114,
    "id": 1,
    "text": "belong to",
    "fromId": 116
},
{
    "toId": 114,
    "id": 2,
    "text": "belong to",
    "fromId": 134
},
{
    "toId": 114,
    "id": 4,
    "text": "belong to",
    "fromId": 136
}
```

```

},
{
  "toId": 114,
  "id": 6,
  "text": "belong to",
  "fromId": 123
},
{
  "toId": 114,
  "id": 8,
  "text": "belong to",
  "fromId": 124
},
{
  "toId": 114,
  "id": 9,
  "text": "belong to",
  "fromId": 126
},
{
  "toId": 114,
  "id": 10,
  "text": "belong to",
  "fromId": 139
},
{
  "toId": 114,
  "id": 11,
  "text": "belong to",
  "fromId": 142
},
{
  "toId": 137,
  "id": 7,
  "text": "belong to",
  "fromId": 114
},
],
"others": [],
"labels": [
{
  "startIndex": 167,
  "endIndex": 182,
  "id": 87,
  "text": "author"
},
{
  "startIndex": 1,
  "endIndex": 37,
  "id": 97,
  "text": "Jornal"
},
{
  "startIndex": 91,
  "endIndex": 168,
  "id": 100,
  "text": "Title"
},
{
  "startIndex": 191,
  "endIndex": 207,
  "id": 102,
  "text": "author"
},
{
  "startIndex": 213,
  "endIndex": 230,
  "id": 103,
  "text": "author"
},
{
  "startIndex": 236,
  "endIndex": 248,
  "id": 104,
  "text": "author"
},
{
  "startIndex": 532,
  "endIndex": 548,
  "id": 109,
  "text": "Publish Date"
},
{
  "startIndex": 347,
  "endIndex": 401,
  "id": 138,
  "text": "Unit"
},
{
  "startIndex": 255,
  "endIndex": 319,
  "id": 140,
  "text": "Unit"
},
{
  "startIndex": 2512,
  "endIndex": 2543,
  "id": 141,
  "text": "doi"
},
{
  "startIndex": 6402,
  "endIndex": 6425,
  "id": 114,
  "text": "Gel composition"
},
{
  "startIndex": 6742,
  "endIndex": 6748,
  "id": 124,
  "text": "Crystallization"
  ↳ "conditions - Temperature #1"
},
{
  "startIndex": 6768,
  "endIndex": 6786,
  "id": 126,
  "text": "Crystallization"
  ↳ "conditions - Time #1"
},
{
  "startIndex": 6159,
  "endIndex": 6165,
  "id": 137,
  "text": "Zeolite"
},
{
  "startIndex": 6565,
  "endIndex": 6583,
  "id": 123,
  "text": "Al#1"
},
{
  "startIndex": 6459,
  "endIndex": 6468,
  "id": 134,
  "text": "H2O Number"
},
{
  "startIndex": 6432,

```

```

    "endIndex": 6442,
    "id": 116,
    "text": "Template Number"
},
{
    "startIndex": 6213,
    "endIndex": 6238,
    "id": 136,
    "text": "P"
},
{
    "startIndex": 6445,
    "endIndex": 6452,
    "id": 139,
    "text": "P Number"
},
{
    "startIndex": 6293,
    "endIndex": 6298,
    "id": 142,
    "text": "Template#1"
}
]
}

```

8.2 Images in data management



Figure E4: Source of data PDF sample.

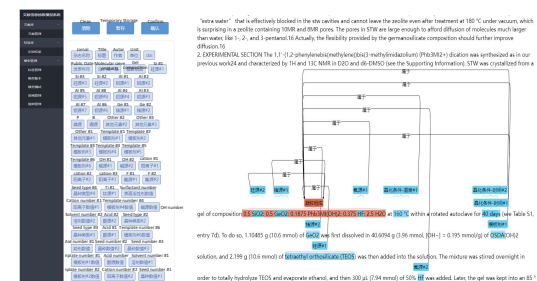


Figure E5: The annotation tools.



Figure E6: An example of dictionary and rule base.

8.3 System Interface

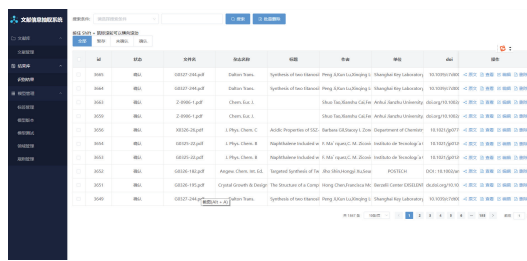


Figure E7: Recognition Result Interface.

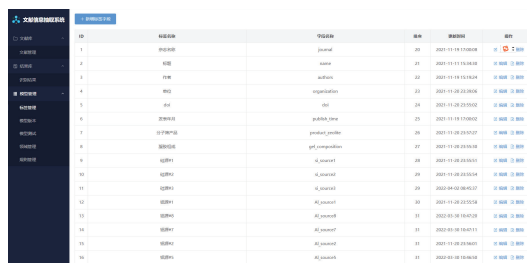


Figure E8: Label Management Page.

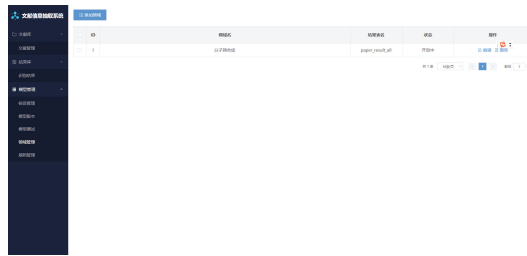


Figure E9: Domain Management Interface.

8.4 Data cross-check code

```
import os
import json

def read_labels(label_path):
    with open(os.path.join(label_path, 'label.txt'), 'r', encoding='utf8') as f_txt:
        return [label.strip() for label in f_txt.readlines()]

def process_json_file(json_path, json_name,
                     labels):
    with open(os.path.join(json_path, json_name), 'r', encoding='utf8') as fp:
        json_data = json.load(fp)

    extracted_data = {label: [] for label in labels}

    for json_item in json_data['labels']:
        for label in labels:
            if label in json_item['text']:
                start = json_item['startIndex']
                end = json_item['endIndex']
                content = json_data['content'][start:end]
                extracted_data[label].append(content)

    return extracted_data

def write_output(new_json_path, extracted_data):
    for label, data in extracted_data.items():
        with open(os.path.join(new_json_path,
                           f'{label}.txt'), 'w', encoding='utf8') as json_file:
            json_file.write(str(data))

def main():
    label_path = ''
    json_path = ''
    new_json_path = ''

    labels = read_labels(label_path)

    all_extracted_data = {label: [] for label in
                         labels}

    for json_name in os.listdir(json_path):
        extracted_data = process_json_file(json_path,
                                         json_name, labels)
        for label, data in extracted_data.items():
            all_extracted_data[label].extend(data)

    write_output(new_json_path, all_extracted_data)

if __name__ == "__main__":
    main()
```

8.5 Label information statistics

Figure E10: Label the DOI information statistics in the data.

Figure E11: Label the Si information statistics in the data.

Figure E12: Label the Gel composition information statistics in the data.